

New experimental measurements and theoretical analysis of the collision-induced absorption in N₂–H₂ pairs

J. Boissoles^a, A. Domanskaya^b, C. Boulet^c, R.H. Tipping^{d,*}, Q. Ma^e

^a*Unite Mixte de Recherche P.A.L.M.S. (Physique des Atomes, Lasers, Molécules, et Surfaces), Université de Rennes I, Campus de Beaulieu, 35042, Rennes Cedex, France*

^b*Institute of Physics, St. Petersburg University, 198504 St. Petersburg, Russia*

^c*Laboratoire de Photophysique Moléculaire, CNRS, Université de Paris-Sud, Centre d'Orsay, Bât 350, 91405 Orsay Cedex, France*

^d*Department of Physics and Astronomy, University of Alabama, P.O. Box 870324, Tuscaloosa, AL 35487, USA*

^e*Department of Applied Physics, Columbia University, and Institute for Space Studies, Goddard Space Flight Center, 2880 Broadway, New York, NY 10025, USA*

Received 26 July 2004; received in revised form 10 December 2004; accepted 10 December 2004

Abstract

We present new experimental data on the collision-induced fundamental absorption in N₂–H₂ mixtures at room temperature and at low enough pressures so that the binary contribution is dominant. Previous measurements have been made at pressures where the ternary and possibly higher absorption coefficients are significant, and this makes it difficult to obtain accurate values for the binary absorption enhancement coefficient. To obtain the enhancement spectrum from the measurements of the mixture, it is necessary to subtract out both the spectra of pure H₂ and N₂, along with some CO₂ impurities thus increasing the experimental uncertainty. Nevertheless, we obtain a value for the integrated intensity of $1.15 \times 10^{-4} \text{ cm}^{-2} \text{ amagat}^{-2}$ that is in good agreement with the previous value of 1.38×10^{-4} . We also discuss how one can scale this result to high temperatures for application to brown dwarf or methane dwarf atmospheres.

© 2005 Elsevier Ltd. All rights reserved.

Keywords: Collision-induced absorption; N₂–H₂ mixtures; High-temperature spectra

*Corresponding author. Tel.: +1 205 348 3799; fax: +1 205 348 5051.

E-mail address: rtipping@bama.ua.edu (R.H. Tipping).

1. Introduction

There exist many astrophysical bodies where N_2 and H_2 are major constituents in their atmospheres. For instances, the planet Mars, the satellites Titan and Triton, and more exotic objects like brown and methane dwarfs. Theoretical atmospheric models of the brown dwarf Gl229B [1] predict that N_2 will dominate over NH_3 at temperatures above 700 K. Like H_2 , the vibration–rotational spectral signatures of N_2 cannot be easily observed because of the lack of allowed dipole transitions. However, it is well known that these homonuclear molecules do absorb radiation through transient dipoles induced during collisions. This process is called collision-induced absorption (CIA) [2], and the resulting spectra differ in several ways from allowed spectra. The intensity of CIA scales quadratically with density and is a function of temperature. The transitions obey different ΔJ selection rules, both molecules in a binary collision can absorb (so-called simultaneous or double transitions), and the widths of the lines are large due to the short duration of collisions. In fact for N_2 , the widths are much larger than the spacing between them so that one only observes the absorption envelope [3].

In the 55 years since CIA was first observed, it is now known to play a major role in the radiative properties of atmospheres, including that of the Earth [2,4]. For this reason, there have been a large number of experimental and theoretical studies of CIA, mostly for diatomic molecules (H_2 , N_2 , and O_2) and for mixtures of these diatomic molecules with rare gases or with each other. A laboratory study of the CIA in N_2 – H_2 in the region of the N_2 fundamental has been made by Reddy and Cho [5]. Other studies in D_2 – N_2 mixtures have been reported as well, but in the region of the D_2 fundamental [6,7]. A number of measurements in the pure rotational region have been reported [8,9]. Measurements of N_2 – H_2 mixtures in the first overtone region at low temperatures have been published by McKellar for possible application to the atmospheres of Titan and Triton [10].

Because of the weakness of the absorption, most of the measurements were carried out at high densities of both gases (up to several hundred amagats). This introduces some uncertainties when extrapolated to low densities or to high temperatures ambient in the atmospheres of brown or methane dwarfs. The first is that at high densities ternary collision cannot be neglected. This implies that the measured absorption does not scale quadratically with the density, either ρ^2 for a pure gas or $\rho_a\rho_b$ for a mixture. The second difficulty is obtaining the enhancement spectra from the measured spectra. One has to subtract out the absorptions of the two pure gases to get the absorption of the pair (the enhancement spectrum). Because the difference in the vibrational constants ω_e for N_2 and H_2 is large, one can easily separate the individual fundamental regions. Also, because the rotational constant B_e for H_2 is about 60 cm^{-1} , simultaneous transitions in which N_2 makes a vibration–rotational transition and H_2 makes a pure rotational transition occur in the far wings of the single transition spectrum where the absorption is small. The situation for D_2 – N_2 mixtures is more complicated for two reasons. The rotational constant B_e for deuterium is approximately $1/2$ that of H_2 so that the double transitions occur closer to the single transitions. The second reason is that the nuclear spin statistics g_J are different for H_2 and D_2 . For H_2 , even rotational states have $g_J = 1$ and odd states have $g_J = 3$, while for D_2 these are 6 and 3, respectively. Thus, the $S_0(0)$ transition in D_2 is stronger and closer to the single transition spectrum than for H_2 , making the subtraction more difficult.

In the present paper, we present some new experimental results for N_2 – H_2 carried out at lower densities where the binary collision approximation is valid. In the following section, we give the experimental details and discuss how the enhancement spectra were obtained. In Section 3, we compare our results with theory, using the zeroth moment of the spectrum that is independent of the line shape of the individual components. We then discuss how we optimize the two parameters appearing in the widely used Birnbaum–Cohen (BC) and extended Birnbaum–Cohen (EBC) [11,12] line shapes in order to fit the observed spectrum. Then in Section 4, we discuss how one can extrapolate our results to higher temperatures occurring in brown and methane dwarf atmospheres. Finally, we draw a few conclusions about refinements of the present work.

2. Experimental details

The FTIR spectra were recorded with a Bruker IFS 120HR instrument equipped with a global source, a KBr beam splitter, and a liquid-nitrogen-cooled MCT detector, by co-adding up to 700 one-sided scans at 0.1 cm^{-1} spectral resolution. A multipass White-type cell fitted with KRS-5 windows was used. The maximum path length obtained was 96 m. The temperature of all the measurements was $22.3 \pm 0.7^\circ\text{C}$, and the maximum pressure of H_2 did not exceed 10 atm, due to limitations of the gas regulator. The spectra obtained were very weak but the absorption was easily detected under these conditions. For analysis, we used the spectrum of the mixture consisting of 1.02 atm of N_2 pressurized by 9.71 atm of H_2 .

To remove any absorption due to H_2 – H_2 pairs, we recorded a spectrum of pure hydrogen at a pressure of 9.8 atm and subtracted this out. There are also collision-induced single and double transitions for N_2 – N_2 pairs, but these are weak because of the approximate 10 to 1 ratio of the number density of H_2 to N_2 . But, in order to improve the accuracy of the enhancement spectrum, we recorded a few spectra of pure N_2 and used the data at 10 atm to subtract out this absorption. There were also some impurity absorption features of CO_2 , and in order to remove these, we calculated the band shape as a sum of Lorentzian lines, using the line parameters from the HITRAN 96 database [13]. After subtraction, only a few weak CO_2 features remain, probably a result of the different broadening coefficients for CO_2 – H_2 and CO_2 –air, which are those listed in HITRAN. The resulting enhancement spectrum is shown in Fig. 1. For reference, we indicate by a stick spectrum the expected positions of some of the S-branch lines of N_2 and H_2 . The two contributions labeled by $n = 1$ and 2 arise from different induction mechanisms as will be discussed in the next section. We note that because of the large rotational constant for H_2 , the absorptions involving a rotational transition in H_2 are well separated from the main absorption feature. As noted above, because of the large widths of the collision-induced lines in comparison with the rotational spacings in N_2 , only a smooth profile is observed.

3. Theoretical analysis

After subtracting out the CIA of H_2 – H_2 , N_2 – N_2 and the CO_2 lines, we obtain the enhancement spectrum denoted $B_0(\omega)$ given by the solid line in Fig. 1. From this profile, we obtain for the experimental binary coefficient, $\alpha_{1b} \equiv \int B_0(\omega) d\omega$, the value $1.15 \times 10^{-4}\text{ cm}^{-2}\text{ amagat}^{-2}$ that is in

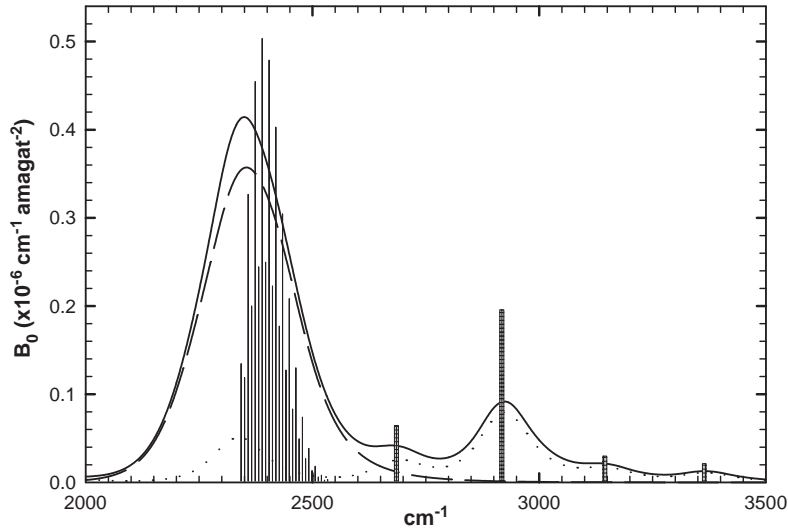


Fig. 1. Enhancement spectrum obtained using 1.02 atm of N_2 and 9.71 atm of H_2 . The total absorption is indicated by the solid line, while the two components, $n = 1$ and 2 as described in the text, are indicated by the dotted and dashed curves, respectively. As a guide, the location of the S-branch lines of N_2 and H_2 are given by a stick spectrum.

good agreement with the value obtained by Reddy and Cho [5] from high-pressure measurements $\alpha_{1b} = (1.38 \pm 0.12) \times 10^{-4} \text{ cm}^{-2} \text{ amagat}^{-2}$. This agreement gives us confidence in our measured spectrum despite the weakness of the absorption and the subtractions necessary to obtain the enhancement spectrum.

As another check on the accuracy of the measured enhancement absorption, we can compare the theoretical and experimental values for the zeroth-moment Γ_0 ; unlike the integrated absorption coefficient, this quantity has a simple sum rule [2] and is independent of the assumed line shape. For the vibrational region where $\coth[\beta\hbar\omega/2] \cong 1$, we can write

$$\Gamma_0 \cong \int B_0(\omega)\omega^{-1} d\omega. \quad (1)$$

The experimental value $\Gamma_0 = 4.6 \times 10^{-8} \text{ amagat}^{-2}$ is in good agreement with the theoretical result assuming only the long-range quadrupolar induction mechanism $\Gamma_0 = 5.12 \times 10^{-8} \text{ cm}^{-1}$. Again, this is reasonable agreement in light of the approximations made and the experimental uncertainties.

From our previous measurements and analyses of the CIA spectra of N_2 – N_2 pairs, we found that most of the absorption in the fundamental region of N_2 arises from the isotropic quadrupolar induction mechanism [14]. There are two distinct contributions labeled by $n = 1$ and $n = 2$ in Fig. 1. The $n = 1$ absorption is proportional to $\alpha_{01}(N_2) Q_{00}(H_2)$, while the $n = 2$ absorption is proportional to $Q_{01}(N_2) \alpha_{00}(H_2)$, where α and Q are the isotropic polarizability and quadrupole moment matrix elements, respectively. The subscripts 00 and 01 refer to pure rotational and fundamental vibrational transitions, and the selection rules for α and Q are $\Delta J = 0$, and $\Delta J = 0, \pm 2$, respectively. From Fig. 1, it is apparent that the absorption for the $n = 2$ mechanism is much larger than that for the $n = 1$ mechanism, except, of course, in the regions corresponding to

rotational transitions in H₂. This is what one would expect from the molecular quadrupole and polarizabilities matrix elements used in our calculations and given in Table 1. One also needs the isotropic interaction potential in order to average over the separation between the centers of mass and we used the one recommended by Borysow and Frommhold [12].

For the first step in fitting the shape of the spectrum, we assume that the line shape for mechanisms 1 and 2 are the same and that there is no vibrational dependence for the shapes. We then calculated the profiles using the BC line shape (the parameter κ in Eq. (13) of Ref. [12] is zero) and the EBC line shape for mechanisms 1 and 2. The results are shown in Fig. 2. From there, one can see that the differences between the BC and EBC are small. Because the anisotropic quadrupolar contributions are also small, in the remaining analysis, we will only consider mechanisms 1 and 2 and we will use the BC line shape.

The calculated spectrum is compared with the experimental data in Fig. 3. It is apparent that calculated peak is too high, so we next optimize the two parameters τ_1 and τ_2 in the BC line shape. Rather than varying them independently, we first calculated the ratio from the values in Ref. [12]

Table 1
Molecular parameters used for the isotropic quadrupole-induction mechanism

Parameter	α_{00} (a_0^3)	α_{01} (a_0^3)	Q_{00} (ea_0^2)	Q_{01} (ea_0^2)
N ₂		0.365 ^a		6.13 × 10 ^{-2a}
H ₂	5.4138 ^b		0.48516 ^c	

^aRef. [16].

^bRef. [17].

^cRef. [18].

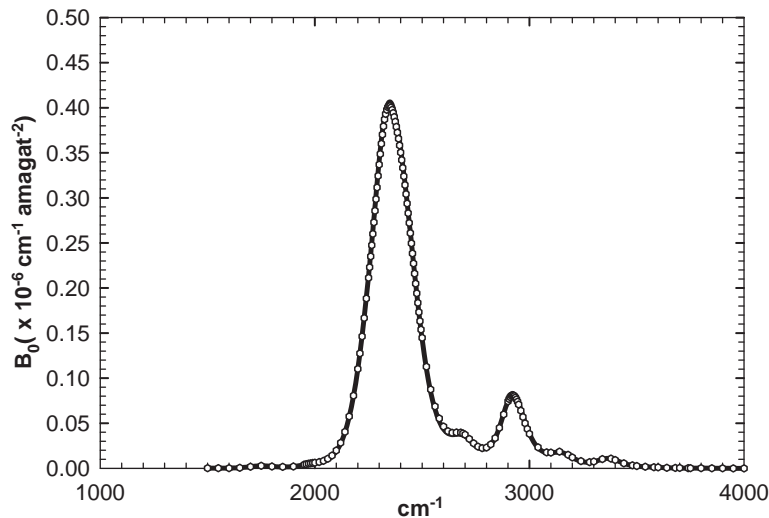


Fig. 2. Comparison of the calculated enhancement spectrum using the $n = 1$ and 2 mechanisms and the ECB model (solid line) and the BC model (triangles).

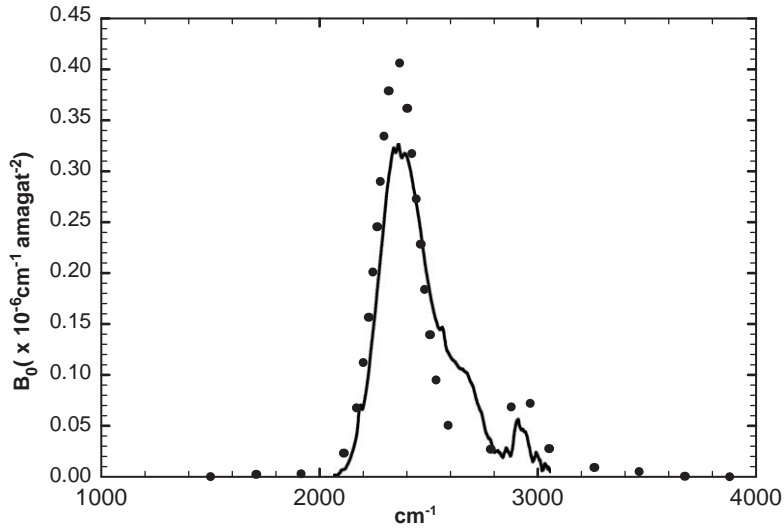


Fig. 3. Comparison of the experimental enhancement spectrum indicated by the solid line with model calculations indicated by dots using the BC line shape with the parameters τ_1 and τ_2 valid for the translation–rotational spectral region.

at 298 K, viz. $\tau_1/\tau_2 = 1.53$. This value is adopted and then we varied τ_1 to obtain a reasonable fit to the shape of the observed spectrum. We found that we could get reasonable agreement if we reduced the value of τ_1 from [12] by the factor 0.7. The comparison between the experiment and the calculated shapes for this choice is shown in Fig. 4. The agreement near the peak of absorption is good, but there are still some differences in the wings where the absorption is weak.

4. Theoretical high-temperature predictions

In this section, we extrapolate the results discussed above to high temperatures for possible application in the model atmospheres of brown dwarfs or methane (T type) dwarfs [15] in the infrared. As mentioned previously, for the two quadrupolar induction mechanisms considered, the zeroth moment has a simple analytic form. Thus, assuming the same isotropic potential used above, we calculate the variation of this moment with T . Results for T between 50 and 2000 K are presented in Fig. 5. Next, we consider the evolution of the line shape with T . The variations of the two parameters, τ_1 and τ_2 , valid for the translation–rotational spectral region for T between 50 and 300 K [12] are shown in Fig. 6. Because τ_1 is related to the duration of collisions, the decrease with increasing T is expected. The T dependence of the ratio τ_1/τ_2 is shown in Fig. 7. From our analysis of the room temperature data, we found that we can get agreement by assuming that the ratio $\tau_1/\tau_2 = 1.53$ and τ_1 for the fundamental region is approximately 0.7 that of Ref. [12]. This is what we will assume for our high-temperature model. To check the consistency of this model, we determined the halfwidth γ of the optimized BC profile at 295 K and obtained $\gamma \cong 90 \text{ cm}^{-1}$. At $T = 1000 \text{ K}$, we find $\gamma \cong 175 \text{ cm}^{-1}$, and the ratio is 1.94. For a given molecular pair, $1/\tau_1 = v/\sigma$,

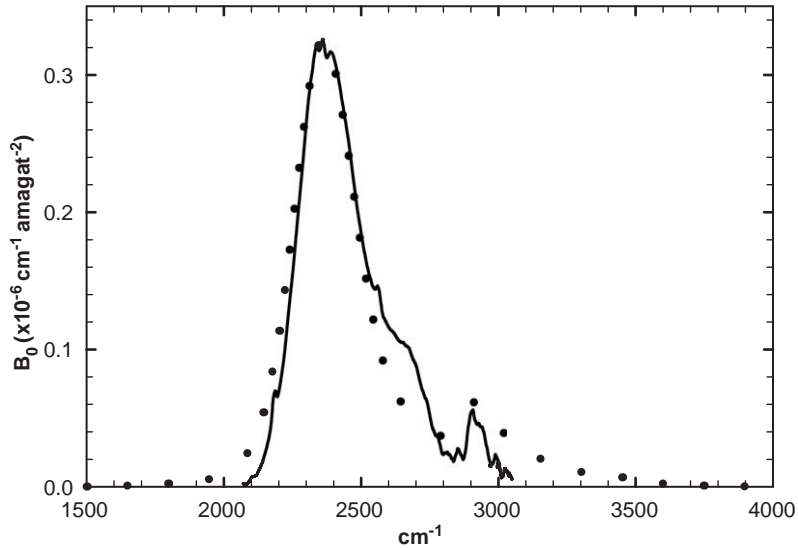


Fig. 4. Comparison between the measured enhancement spectrum and the calculated spectrum using the optimized value $0.7\tau_1$ for the fundamental region.

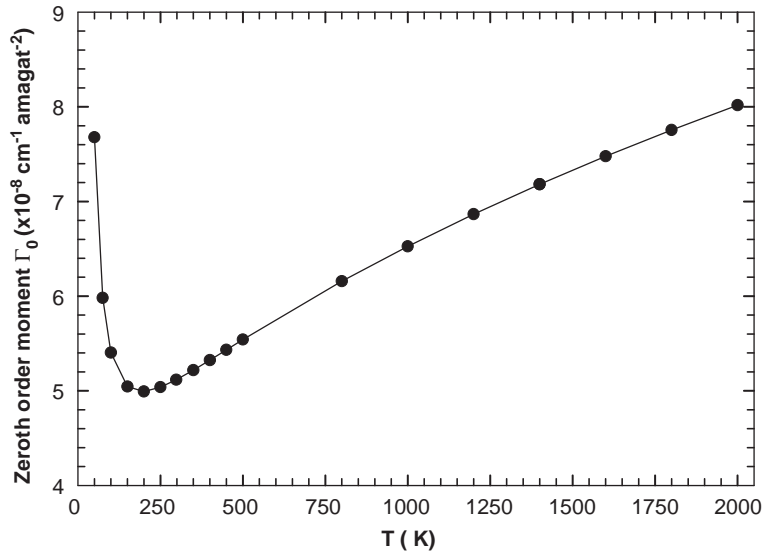


Fig. 5. Dependence of the zeroth moment Γ_0 with temperature.

where v is the relative speed between the pair and σ is a characteristic distance such as the Lennard Jones radius. Using the equipartition theorem, $v = (3kT/m)^{1/2}$, where m is the reduced mass of the pair, and from the uncertainty principle $\gamma \propto 1/\tau_1$, so that $\gamma \propto (T/m)^{1/2}$. This gives the ratio of 1.84 that is not too different from the value we found above.

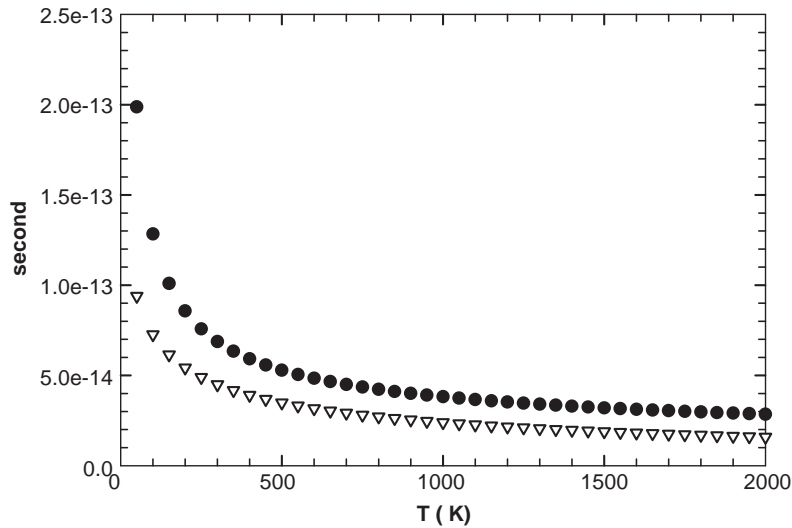


Fig. 6. Variation of the parameter τ_1 (dots) and τ_2 (triangles) from [12] with temperature.

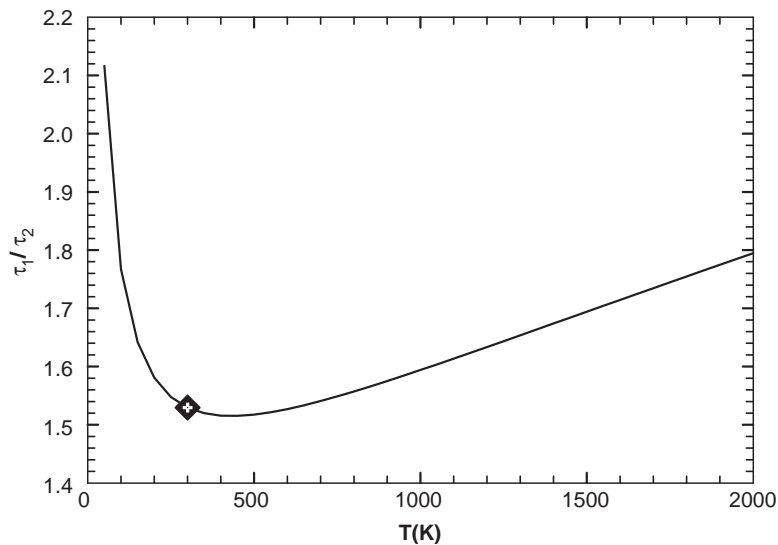


Fig. 7. Variation of the ratio τ_1/τ_2 from [12] with temperature; the value obtained by fitting the room temperature experimental results is indicated.

As another check, we can compare the halfwidths obtained for the fundamental band region for $\text{N}_2\text{-D}_2$ pairs at $T = 298$ K with the value for $\text{N}_2\text{-H}_2$ at $T = 295$ K. We find that $\gamma(\text{N}_2\text{-H}_2) = 1.36\gamma(\text{N}_2\text{-D}_2)$. Using the recent value from Ref. [7], $\gamma(\text{N}_2\text{-D}_2) = (70.7 \pm 2.7) \text{ cm}^{-1}$, we obtain the value $\gamma(\text{N}_2\text{-H}_2) = (96.3 \pm 3.7) \text{ cm}^{-1}$ that is in very good agreement with our value. Finally, knowing the T dependence of the zeroth moment and the line shape, we can calculate the absorption at temperatures of interest. As a typical example, we present in Fig. 8 the spectrum at $T = 1000$ K; similar results are easily generated for other T .

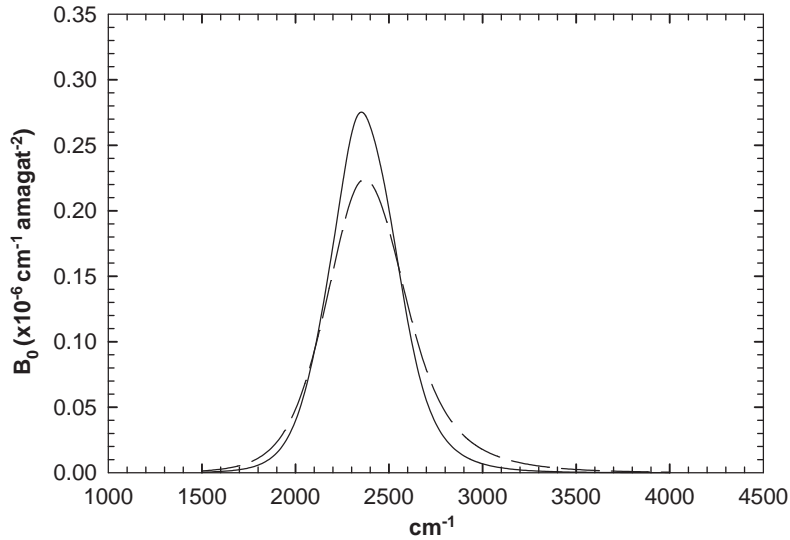


Fig. 8. Predicted spectrum calculated for $T = 1000$ K; the solid curve is the result using the parameters τ_1 and τ_2 from [12] while the dashed curve uses the optimized values as described in the text.

5. Conclusions

In the present work, we have made a number of simplifying theoretical approximations justified by the experimental uncertainties in the measurement of the weak collision-induced enhancement spectrum. First, we only included the quadrupolar induction mechanism. There are higher multipolar mechanisms that satisfy different rotational selection rules. For instance, the hexadecapolar mechanism that also allows $\Delta J = 4$ transitions would result in additional absorption in the wings of the band. In calculating the average over the separation R between the centers of mass, we used only the isotropic part of the interaction potential. One can use an anisotropic potential, but this complicates the calculations because one cannot calculate the resulting absorption as a superposition of independent contributions. Furthermore, for the quadrupolar induction mechanism, we used only the leading long-range part of the induced dipole; all the various components have a short-range part that varies exponentially with R . For calculations in $\text{H}_2\text{--H}_2$ pairs where the experimental data is more accurate than in the present case, and ab initio calculations of the various induced dipoles are known [2], these can affect the corresponding absorption significantly. We have also arbitrarily adjusted the line shape used to account for the (unknown) vibrational dependence, and adopt a simple temperature-dependent scaling. Nevertheless, the high-temperature results are expected to provide adequate accuracy for inclusion in atmospheric models. Of course, with the availability of more accurate laboratory data, or accurate ab initio induced dipole moment components and line shapes, one can easily refine the theoretical model and predictions. Finally, we note that one can easily generalize the method used here to other collisional pairs of interest.

Acknowledgments

Two of the authors (RT and QM) would like to acknowledge support from the Planetary Atmospheres Program of NASA through Grant NAG5-13337. Another (AD) would like to acknowledge support from the Russian Foundation for Basic Research (RFBR).

References

- [1] Burrows A, Hubbard WB, Lunine JI, Liebert L. The theory of brown dwarfs and extrasolar planets. *Rev Mod Phys* 2001;73:719–65.
- [2] Frommhold L. Collision-induced absorption in gases. Cambridge: Cambridge University Press; 1993.
- [3] Boissoles J, Boulet C, Tipping RH, Brown A, Ma Q. Theoretical calculation of the translation–rotation collision-induced absorption in N_2 – N_2 , O_2 – O_2 and N_2 – O_2 pairs. *J Quant Spectrosc Radiat Transfer* 2004;82:505–16 and references therein.
- [4] Rich N, McKellar ARW. A bibliography on collision-induced absorption. *Can J Phys* 1976;54:486; Hunt JL, Poll JD. A second bibliography on collision-induced absorption. *Mol Phys* 1986;59:163.
- [5] Reddy SP, Cho CW. Induced infrared absorption of nitrogen and nitrogen–foreign gas mixtures. *Can J Phys* 1965;43:2331–43.
- [6] Pai ST, Reddy SP, Cho CW. Induced infrared absorption of deuterium in deuterium–foreign gas mixtures. *Can J Phys* 1974;52:72–81.
- [7] Varghese G, Stamp C, Reddy SP. Collision-induced fundamental band of D_2 in D_2 – N_2 and D_2 –CO mixtures. *J Quant Spectrosc Radiat Transfer* 2004;87:387–97.
- [8] Dore P, Borysow A, Frommhold L. Roto-translational far-infrared absorption spectra of H_2 – N_2 pairs. *J Chem Phys* 1986;84:5211–3.
- [9] Codasfano P, Dore P. Far infrared absorption of N_2 – H_2 gaseous mixtures. *J Quant Spectrosc Radiat Transfer* 1986;36:445–52.
- [10] McKellar ARW. Low-temperature infrared absorption of gaseous N_2 and $N_2 + H_2$ in the 2.0–2.5 μm region: application to the atmospheres of Titan and Triton. *Icarus* 1989;80:361–9.
- [11] Birnbaum G, Cohen ER. Theory of line shape in pressure-induced absorption. *Can J Phys* 1976;54:593–602.
- [12] Borysow A, Frommhold L. Theoretical collision-induced rototranslational absorption spectra for modeling Titan’s atmosphere: H_2 – N_2 pairs. *Ap J* 1986;309:495–510.
- [13] Rothman LS, Rinsland CP, Goldman A, Massie ST, Edwards DP, Flaud J-M, Perrin A, Camy-Peyret C, Dana V, Mandin J-Y, Schroeder J, McCann A, Gamache RR, Wattson BB, Yoshino K, Chance KV, Jucks K, Brown LR, Nemtchinov V, Varanasi P. The HITRAN molecular spectroscopic database and HAWKS (HITRAN Atmospheric Workstation): 1996 edition. *J Quant Spectrosc Radiat Transfer* 1998;60:665–710.
- [14] Boissoles J, Tipping RH, Boulet C. Theoretical study of the collision-induced fundamental absorption spectra of N_2 – N_2 pairs for temperatures between 77 and 297 K. *J Quant Spectrosc Radiat Transfer* 1994;51:615–27.
- [15] Burgasser AJ, Kirkpatrick JD, Brown ME, Reid IN, Gizis JE, Dahn CC, Monet DG, Beichma CA, Liebert J, Cutri RM, Skrutskie MF. Discovery of four field methane (T-type) dwarfs with the two micron all-sky survey. *Ap J* 1999;522:L65–8.
- [16] Moreau G, Boissoles J, Le Doucen R, Boulet C, Tipping RH, Ma Q. Experimental and theoretical study of the collision-induced fundamental spectra of N_2 – O_2 and O_2 – N_2 pairs. *J Quant Spectrosc Radiat Transfer* 2001;69:245–56.
- [17] Hunt JL, Poll JD, Wolniewicz L. Ab initio calculation of properties of the neutral hydrogen molecules H_2 , HD, D_2 , DT and T_2 . *Can J Phys* 1984;62:1719–23.
- [18] Poll JD, Wolniewicz L. The quadrupole moment of the H_2 molecule. *J Chem Phys* 1978;68:3053–8.